ACTA IMEKO
ISSN: 2221-870X
December 2026, Volume 15, Number 4, 1 – 8

Tensile and shear performance of polyurethane foam joints in masonry after short-term natural environmental exposure

Erik Kovaček[1], Emina Hadžalić[1], Nina Čeh[1]

[1] *University of Rijeka, Faculty of Civil Engineering, Radmile Matejčić 3, 51000 Rijeka, Croatia*

ABSTRACT
This study investigates the mechanical behaviour of polyurethane (PU) foam joints in masonry, with a focus on tensile and shear performance following short-term natural environmental exposure. Test specimens were prepared using precision-ground clay masonry blocks bonded with a one-component PU adhesive, forming thin-layer joints. Two groups were considered: a reference series maintained under controlled laboratory conditions and an exposed series subjected to unsheltered natural outdoor conditions for 33 days. All tests were conducted under quasi-static, displacement-controlled conditions. Compared with the reference specimens, the exposed series showed lower mean peak loads, with reductions of approximately $31\,\%$ in tension and $29\,\%$ in shear. Owing to the limited number of specimens and the short exposure period, these results are interpreted as preliminary evidence of environmental sensitivity rather than as an assessment of long-term durability. The study provides experimental data for the further characterisation and modelling of thin PU adhesive joints in masonry systems.

Section: RESEARCH PAPER

Keywords: masonry; PU foam joints; tensile performance; shear performance; short-term environmental exposure

Citation: E. Kovaček, E. Hadžalić, N. Čeh, Tensile and shear performance of polyurethane foam joints in masonry after short-term natural environmental exposure, Acta IMEKO, vol. 15 (2026) no. 4, pp. 1–8. DOI: 10.21014/actaimeko.v15i4.2498

Section Editor: Francesco Lamonaca, University of Calabria, Italy

Received: August 24, 2026; **In Final Form:** November 16, 2026; **Published:** December 2026.

Copyright: This is an open-access article distributed under the terms of the Creative Commons Attribution 4.0 International License.

Funding: This work has been supported by the Croatian Science Foundation under project Resilient Engineering of Ductile Bonded Masonry: Understanding Dynamic Behavior and Seismic Response Across Scales (ResiBOND, HRZZ-UIP-2025-02-2749), Croatia.

Corresponding Author: Nina Čeh, e-mail: nina.ceh@uniri.hr

1. INTRODUCTION

The increasing demand for faster and more efficient construction methods has encouraged the development of alternative bonding techniques in masonry, such as thin-joint systems [1]–[3]. Conventional cement-based mortars, although widely established, are associated with several limitations, including time-consuming installation, variability in material properties, and strong dependence on workmanship. Their performance is influenced by factors such as mixing quality, water content, and curing conditions, which may lead to inconsistencies in mechanical behaviour and long-term durability.

In recent years, polyurethane (PU) foam adhesives have been introduced as a modern bonding solution. Unlike traditional mortars, these systems are applied as thin adhesive layers without the need for mixing or water, enabling faster and cleaner construction processes [4], [5]. In addition to improving productivity, PU-based joints contribute to reduced thermal bridging due to their low thermal conductivity [4].

Despite these advantages, the structural performance of PU foam joints remains insufficiently understood. Previous studies have shown that masonry bonded with PU adhesives may exhibit lower compressive strength and stiffness compared to conventional systems [5]–[8], while achieving comparable or even improved behaviour under tensile and shear loading [5], [8]. In addition, PU-bonded masonry has been reported to exhibit increased ductility and enhanced energy dissipation capacity [7], which is particularly beneficial for structures located in seismic-prone regions. However, the performance of PU-based adhesives is also influenced by environmental factors, including temperature and moisture, which may affect joint strength and long-term durability [9]–[11]. Considering that masonry structures are exposed to varying environmental actions during their service life, such exposure may affect the mechanical behaviour and durability of polyurethane-based joints. In this context, previous experimental studies have investigated the influence of temperature variations on the adhesion strength of masonry bonded with PU foam [12], while longer-term hygrothermal and outdoor ageing studies on structural polyurethane adhesives have also reported changes in mechanical properties [11].

The successful application of PU foam adhesives in masonry construction requires sufficient bond strength at the interface with masonry units. The bond performance is governed by the



Figure 1. Porotherm 25 S block.

properties of the adhesive, the type and characteristics of the masonry units, and the quality of workmanship during installation [13]. The present study aims to experimentally investigate the mechanical behaviour of polyurethane foam joints in masonry, with a focus on tensile and shear response. The experimental programme is based on specimens composed of precision-ground clay blocks bonded with a one-component PU foam adhesive, forming thin joints of controlled thickness. Special attention is given to the influence of environmental exposure on joint performance by comparing specimens maintained under controlled laboratory conditions with those subjected to natural atmospheric conditions. The results provide insight into the mechanical performance of polyurethane-based joints, contributing to a better understanding of their applicability in modern masonry construction.

2. EXPERIMENTAL PROGRAMME

The experimental programme comprised tensile and shear tests on PU-bonded clay masonry specimens. For each loading configuration, six specimens were tested: three reference specimens maintained under laboratory conditions and three specimens subjected to 33 days of unsheltered natural outdoor exposure. All specimens were manufactured using the same masonry units, adhesive product and application procedure. The following sections describe the specimen geometry, exposure conditions, loading configurations, and measurement procedures.

2.1. Materials and specimens

For the preparation of test specimens, Porotherm 25 S blocks, manufactured by Wienerberger, were used as adherends. The blocks, shown in Figure 1, have nominal dimensions of $375 \times 250 \times 238\,\mathrm{mm}^3$, providing a standard wall thickness of 25 cm. These precision-ground masonry units are characterised by high dimensional accuracy, which enables their assembly using thin-layer bonding materials, such as specialised mortars or polyurethane adhesive systems. The bonding material used in this study was a commercially available one-component polyurethane foam adhesive specifically developed for masonry construction, which allows masonry joints to be produced without water, mixing, or traditional mortar preparation processes.

Test specimens were prepared by applying the polyurethane foam between two brick units, forming thin joints with a nominal thickness below 1 mm. Owing to the high dimensional precision of the blocks, geometric variability of the bed surfaces was reduced compared with conventional masonry units. Although masonry blocks inherently exhibit a certain level of material heterogeneity, their geometric consistency contributed to repeatable specimen preparation.

Specimen preparation was carried out in accordance with the manufacturer's guidelines and standard laboratory practices for testing masonry joints. Porotherm 25 S units were cleaned of dust and debris prior to bonding to promote consistent adhesion. The

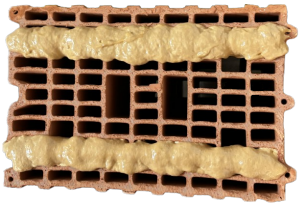


Figure 2. Brick specimen following polyurethane foam applications.



(a) (b)

Figure 3. Tensile test specimen.

polyurethane adhesive Dryfix was applied using a calibrated applicator in the form of two continuous parallel beads along the horizontal bed surface, following the manufacturer's recommended application pattern, as illustrated in Figure 2. Particular care was taken to ensure consistent application, followed by immediate placement and slight pressing of the blocks. This procedure was adopted to reduce preparation-induced variability between specimens.

For each loading configuration (tensile and shear), six specimens were prepared and tested, comprising three reference and three exposed samples.

2.1.1. Tensile test specimens

The tensile response of the joints between the clay blocks and the polyurethane foam was evaluated using a test configuration in which the upper block was supported, whereas the lower block was suspended and subjected to loading, with the load transmitted through the bonded interface, as illustrated in Figure 3. This arrangement was intended to produce predominantly tensile loading within the adhesive layer.

For comparison between specimens, two stress measures were considered. The first is a gross projected-area nominal stress based on the full geometric overlap of the masonry units,

$$\sigma_{\mathrm{t,gross},i} = \frac{F_{i,\max}}{A_{\mathrm{gross,t}}}, \tag{1}$$

where, because one block was rotated by 90° relative to the other, $A_{\mathrm{gross,t}} = 250\,\mathrm{mm} \times 250\,\mathrm{mm} = 62\,500\,\mathrm{mm}^2$. This gross projected area is not the actual PU–masonry bonded area because the masonry units are perforated and the adhesive was applied in two discrete beads. The corresponding stress is therefore retained only as a nominal system-level reference and must not be interpreted as the tensile strength of the tested joint.

A second stress measure was calculated using the effective bonded area. The actual adhesive footprint observed on the masonry surface for one specimen was transferred to the known block geometry and vectorised. Only the adhesive-covered portions of solid ceramic material located within the $250\,\mathrm{mm} \times 250\,\mathrm{mm}$ overlap region were included. This procedure resulted in an effective

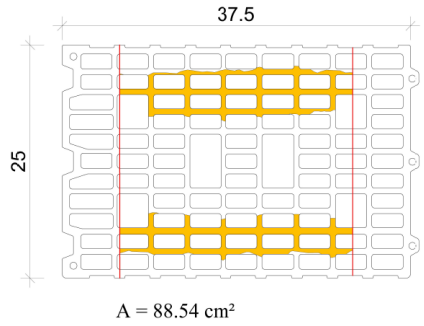
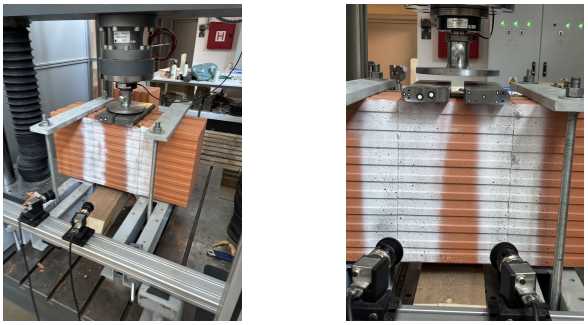


Figure 4. Determination of the effective bonded area for the tensile-test configuration.



(a) (b)

Figure 5. Shear test specimen.

bonded area of $A_{\mathrm{eff,t}} = 8854\,\mathrm{mm}^2$ ($88.54\,\mathrm{cm}^2$). The effective bonded-area tensile stress was calculated as

$$\sigma_{\mathrm{t,eff},i} = \frac{F_{i,\max}}{A_{\mathrm{eff,t}}}. \tag{2}$$

The effective area represents an image- and geometry-based estimate of the load-transferring PU–masonry interface; specimen-to-specimen variations in the adhesive footprint were not quantified individually. The effective bonded area used for the tensile-stress calculation is shown in Figure 4.

2.1.2. Shear test specimens

The shear response of the joints between the clay blocks and the polyurethane foam was evaluated using a three-block assembly arranged vertically. The adopted geometry follows the general three-unit shear arrangement; however, the present configuration was adapted for the PU-bonded specimens and was not intended as a determination of initial shear strength according to the standard. The load was applied to the central block through a compression plate, while the outer blocks acted as supports, as shown in Figure 5. This configuration induced predominantly shear loading within the adhesive layers, resulting in relative sliding between the bonded elements. To minimise the rotation of the outer blocks and to approximate a shear-dominated stress state, the lateral elements were additionally restrained. However, due to the geometry of the masonry units and the complexity of force transfer, minor rotations occurred during testing, influencing the stress distribution within the joints. Despite these effects, the adopted configuration provided useful comparative information on the shear behaviour of the polyurethane adhesive joints.

As for the tensile tests, two stress measures were considered. The gross projected area of one shear joint was $A_{\mathrm{gross,s}} = 375\,\mathrm{mm} \times 250\,\mathrm{mm} = 93\,750\,\mathrm{mm}^2$, and the corresponding nominal shear stress was calculated as

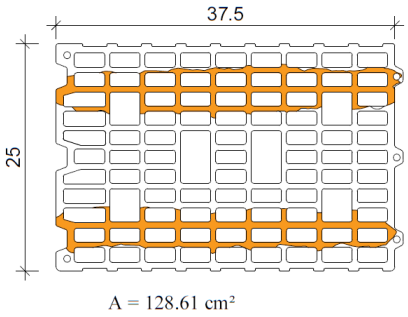


Figure 6. Determination of the effective bonded area for one shear plane.

$$\sigma_{\mathrm{s,gross},i} = \frac{F_{i,\max}}{2\,A_{\mathrm{gross,s}}}, \tag{3}$$

where the factor 2 accounts for the two shear planes. As in the tensile tests, this gross-area quantity does not represent the stress transferred through the actual PU–masonry interface and is retained only as a nominal system-level reference.

The effective bonded area was obtained by vectorising the actual adhesive footprint on the perforated masonry bed surface and excluding the void regions. The resulting effective bonded area was $A_{\mathrm{eff,s}} = 12\,861\,\mathrm{mm}^2$ ($128.61\,\mathrm{cm}^2$) for one joint. The effective bonded-area shear stress was therefore calculated as

$$\sigma_{\mathrm{s,eff},i} = \frac{F_{i,\max}}{2\,A_{\mathrm{eff,s}}}. \tag{4}$$

The same effective area was used for all specimens because individual specimen-to-specimen variations in the adhesive footprint were not quantified. The effective bonded area used for the shear-stress calculation is shown in Figure 6.

2.2. Environmental conditions and short-term exposure

The reference series specimens were maintained under controlled laboratory conditions at a temperature of 20 °C and relative humidity (RH) of 50 %. The exposed series specimens were subjected to natural environmental conditions from July 25 to August 26, 2025. During this period, the samples were placed outdoors without protection and were directly exposed to temperature variations, solar exposure, and precipitation. The purpose of this exposure was to investigate the short-term response of the bonded joints to unsheltered natural outdoor conditions rather than to reproduce a specific long-term service environment. The environmental conditions recorded during this period (Figure 7) are representative of a summer period in the Adriatic region, characterised by thermal fluctuations and intermittent rainfall.

During the observed exposure period, the average air temperature was 25.1 °C, while the maximum recorded temperature reached 37.2 °C, and the minimum temperature dropped to 13.3 °C, as shown in Figure 7. Over the total exposure duration of 33 days, precipitation occurred on 9 days, with a cumulative rainfall amount of 112.5 mm. The specimens were therefore subjected to a combined outdoor exposure involving temperature variation, moisture, and solar exposure. Since solar irradiance was not measured separately, the individual contribution of solar or UV radiation cannot be isolated from the combined environmental action. The comparison between the exposed and reference series is therefore interpreted as an assessment of short-term environmental sensitivity rather than long-term durability.

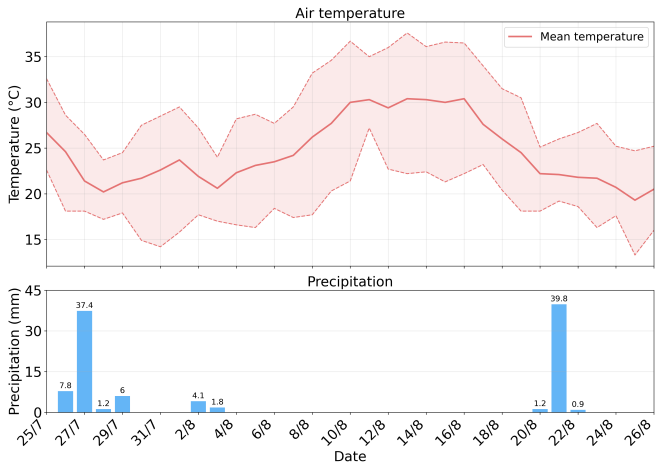


Figure 7. Meteorological conditions during the exposure period.

2.3. Testing equipment and measurement techniques

All tensile and shear tests were conducted under quasi-static, displacement-controlled conditions using a Zwick Roell Z600 testing machine located at the Laboratory for Structures, Faculty of Civil Engineering, University of Rijeka, with a maximum capacity of 600 kN. For the purposes of this study, the lower testing module was used with appropriate fixtures and adaptations up to 50 kN, which was sufficient for all test series. Special loading fixtures, support plates, and hinged bases were employed to promote proper load transfer and alignment during testing. The global displacement reported by the testing machine was obtained from the crosshead of the Zwick Roell Z600. Consequently, this measurement represents the displacement of the loading system and includes the deformation of the specimen, together with the compliance of the loading fixtures and other components located within the load path.

During shear testing, full-field displacements and deformations were additionally monitored using a GOM Aramis 3D 12M optical system based on digital image correlation (DIC) [14]. DIC has also been applied to the analysis and identification of masonry triplet shear behaviour [15]. Prior to testing, the specimen surfaces were prepared with a random black-and-white speckle pattern to provide sufficient contrast for optical tracking, as shown in Figure 5. The acquired images were processed using GOM Correlate software. For the shear-test DIC evaluation, two pairs of virtual measurement points were selected on the front surface of the masonry units immediately adjacent to each adhesive joint, with the points in each pair positioned on opposite sides of the joint. For each pair, the relative displacement of the two masonry units was calculated using the displacement component parallel to the direction of the applied load. The displacement of each joint was defined as the arithmetic mean of the relative displacements obtained from the two point pairs. For the three-block shear specimens, the same procedure was applied to both adhesive joints, and the reported DIC displacement was calculated as the arithmetic mean of the displacements obtained for the two joints. Such measurements were not performed during tensile testing due to limited visibility and restricted optical access to the joint.

All tests were performed under displacement control at a constant loading rate of 0.2 mm/min. The testing-machine signals were recorded at a sampling frequency of 2000 Hz, while the DIC images were acquired at 1 fps.

For the construction of the mean force–displacement curves, the individual curves within each series were referenced to a common zero-displacement origin and linearly interpolated onto a common displacement grid. The mean response was then obtained by calculating the arithmetic mean of the force values at each displacement point within the displacement range common to all specimens of the corresponding series.

Table 1. Peak load, gross-area nominal tensile stress, and effective bonded-area tensile stress of all tested specimens.

	TR-1	TR-2	TR-3	TE-1	TE-2	TE-3
Peak load in kN	9.77	10.90	13.65	7.06	6.30	10.22
Gross nominal stress in MPa	0.156	0.174	0.218	0.113	0.101	0.164
Effective bonded stress in MPa	1.103	1.231	1.542	0.797	0.712	1.154

Table 2. Mean and sample standard deviation of individual tensile-test peak values.

Series	Peak load in kN	Gross in MPa	Effective in MPa
Reference series	11.44 ± 2.00	0.183 ± 0.032	1.292 ± 0.225
Exposed series	7.86 ± 2.08	0.126 ± 0.033	0.888 ± 0.235

3. EXPERIMENTAL RESULTS

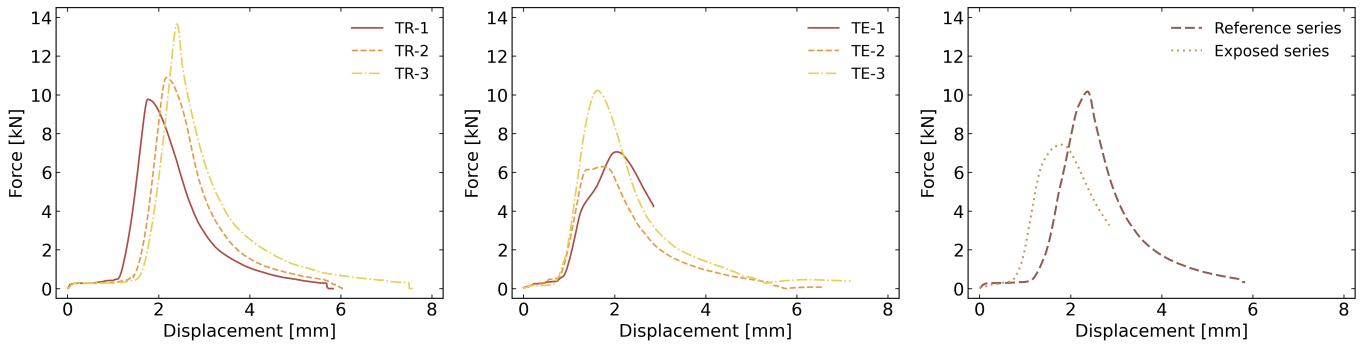
3.1. Tensile tests

The tensile test results indicate a nonlinear mechanical response of the PU foam joints, characterised by an initial increase in load-bearing capacity followed by a softening behaviour after reaching the peak force. The force–displacement curves obtained for the reference and exposed series are presented in Figure 8a and Figure 8b, respectively.

The peak load, gross-area nominal stress and effective bonded-area stress values for all individual specimens are summarised in Table 1. Among the reference specimens, TR-3 achieved the highest peak load of 13.65 kN, while the exposed specimens generally exhibited lower peak values, with TE-2 showing the lowest resistance of only 6.30 kN. The exposed specimens generally exhibited lower tensile resistance than the reference specimens. Because the exposure involved combined temperature variation, moisture and solar exposure, the present tests do not allow the contribution of individual environmental actions or degradation mechanisms to be isolated.

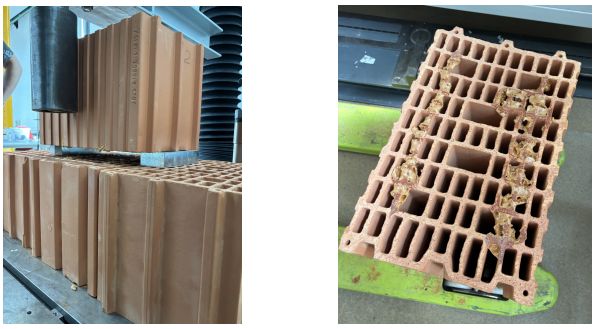
In order to facilitate comparison between the two groups, mean response curves were determined from the individual test results and are presented in Figure 8c. The comparison of the mean responses indicates a broadly similar initial response for both specimen groups, whereas differences become more pronounced at higher load levels. For quantitative comparison, Table 2 reports the mean and sample standard deviation of the individual peak loads and corresponding nominal tensile stresses. The reference series reached a mean peak load of 11.44 kN, while the exposed series reached 7.86 kN, corresponding to a reduction of approximately 31 %. Given the limited number of specimens ($n = 3$ per series), these differences are interpreted descriptively and no claim of statistical significance is made.

Despite the reduction in resistance observed in the exposed series, the overall shape of the force–displacement curves remained similar for both groups, suggesting that short-term environmental exposure primarily affected load-carrying capacity rather than producing a clearly different macroscopic response. The post-peak response is characterised by gradual degradation of load-carrying capacity, consistent with progressive damage development and softening within the polyurethane adhesive layer after crack initiation. Visual inspection of the tested specimens indicated predominantly cohesive failure within the adhesive layer, using terminology consistent with the general failure-pattern classification for



(a) Reference series (b) Exposed series (c) Mean curves

Figure 8. Results of tensile tests obtained from the testing machine.



(a) (b)

Figure 9. Representative failure surface of a PU foam joint after tensile test.

bonded assemblies. A representative failure surface after tensile testing is presented in Figure 9.

It should again be noted that DIC measurements were not performed during tensile testing due to limited visibility and restricted optical access to the specimen configuration, which prevented reliable tracking of the relative displacement within the adhesive layer independently of the global compliance and displacement of the testing system.

3.2. Shear tests

The force–displacement curves obtained from the testing machine during the shear tests for the reference and environmentally exposed series are presented in Figure 10a and Figure 10b, respectively, while the corresponding mean response curves are shown in Figure 10c. Similar to the tensile tests, the reference series exhibited higher load-bearing capacity compared to the exposed specimens.

The peak load, gross-area nominal shear stress, and effective bonded-area shear stress values obtained for all individual specimens are summarised in Table 3. Among the reference specimens, SR-2 achieved the highest peak load of 22.37 kN, followed by SR-3 with 20.58 kN, whereas the exposed specimens generally exhibited lower load-bearing capacities. The lowest peak load was recorded for specimen SE-3, which reached 12.74 kN. Based on the individual peak values, the reference series reached a mean peak load of 19.26 kN, while the exposed series reached 13.73 kN, corresponding to a reduction of approximately 29 %. The mean values and sample standard deviations are summarised in Table 4.

The observed reduction in shear resistance is consistent with the trend identified in the tensile tests. Based on the mean of the individual specimen peak loads, the tensile tests showed a reduction of approximately 31 %, while the shear tests showed a reduction of approximately 29 %. Both loading configurations

Table 3. Peak load, gross-area nominal shear stress and effective bonded-area shear stress of all tested specimens.

	SR-1	SR-2	SR-3	SE-1	SE-2	SE-3
Peak load in kN	14.84	22.37	20.58	15.04	13.42	12.74
Gross nominal stress in MPa	0.079	0.119	0.110	0.080	0.072	0.068
Effective bonded stress in MPa	0.577	0.870	0.800	0.585	0.522	0.495

Table 4. Mean and sample standard deviation of individual shear-test peak values.

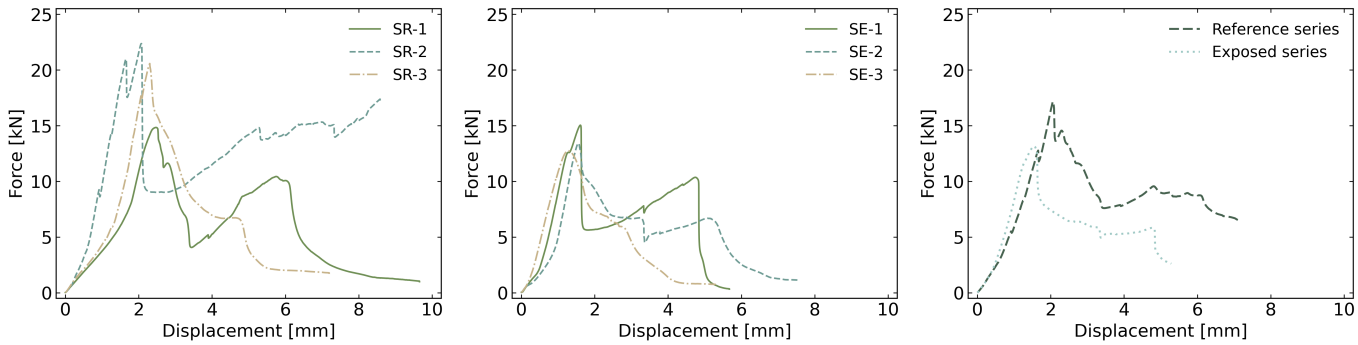
Series	Peak load in kN	Gross in MPa	Effective in MPa
Reference series	19.26 ± 3.93	0.103 ± 0.021	0.749 ± 0.153
Exposed series	13.73 ± 1.18	0.073 ± 0.006	0.534 ± 0.046

therefore exhibited lower mean peak resistance after the short-term outdoor exposure. Given the small number of specimens, these results should be regarded as preliminary descriptive trends rather than evidence of statistical significance.

The deformation of the specimen during the shear test is illustrated in Figure 11. It should be noted that the applied shear configuration was influenced by minor rotations of the masonry units during loading. Although the outer blocks were additionally restrained in order to minimise rotational effects and approximate a pure shear stress state, the geometry of the masonry units and the complexity of force transfer resulted in localised rotations and a nonuniform stress distribution within the adhesive layer. These effects are reflected in the irregularities and fluctuations observed in certain force–displacement curves, particularly in the post-peak region.

In addition to the global response recorded by the testing machine, the shear tests were additionally analysed using DIC, which enabled monitoring of local displacements and deformation development within the adhesive layer during loading. Unlike the machine measurements, which represent the overall displacement of the testing system, the DIC analysis enabled direct monitoring of the relative displacement between the bonded masonry units in the vicinity of the adhesive layer.

The force–displacement curves obtained from the DIC analysis are presented in Figure 12a and Figure 12b for the reference and exposed series, respectively, while the corresponding mean DIC-based response curves are shown in Figure 12c. The mean DIC-based response curves for the reference and exposed series show a broadly similar initial response. Differences become more pronounced in the peak-load region and during the post-peak response, where the exposed specimens show lower peak resistance and reduced deformation capacity compared with the reference series.



(a) Reference series (b) Exposed series (c) Mean curves

Figure 10. Results of shear tests obtained from the testing machine.



(a) (b)

Figure 11. Deformation of the specimen during shear test.

A comparison between the mean force–displacement curves obtained from the testing machine and the DIC analysis is presented in Figure 13.

The displacement obtained from the testing machine represents the global displacement of the loading system and therefore includes not only deformation of the adhesive joint but also compliance of the loading frame, fixtures and support system. Additional contributions may arise from local contact deformation or indentation of the masonry units at the loading and support points, as well as from minor rotations and eccentricities of the specimen during loading. In contrast, the DIC measurement was defined from the relative displacement of regions located on the masonry units immediately adjacent to the adhesive layer and therefore excludes most of the deformation occurring outside the joint region. Consequently, the DIC-based curves show a stiffer apparent response and provide a more local measure of joint deformation, whereas the machine displacement represents the response of the complete specimen–fixture–machine system.

3.3. Effect of short-term environmental exposure

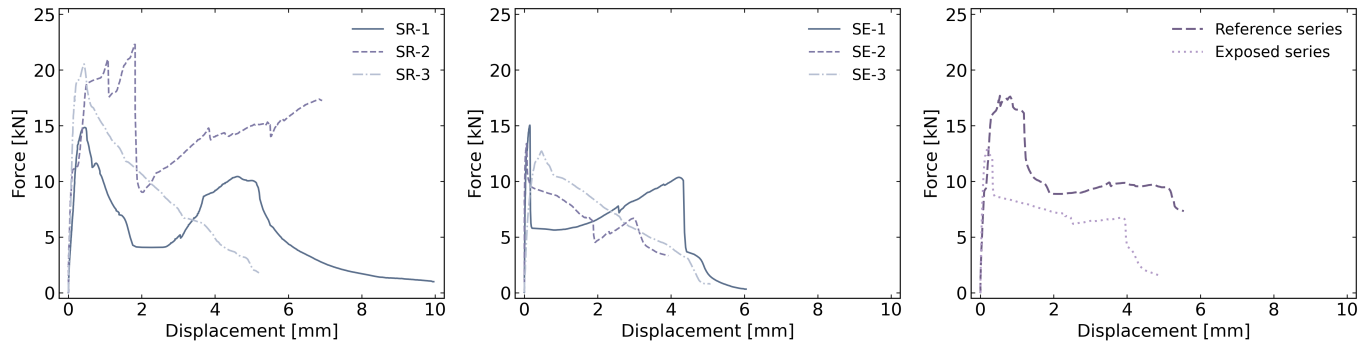
The tensile and shear tests showed a consistent reduction in mean peak resistance after 33 days of unsheltered natural outdoor exposure. The mean tensile peak load decreased from 11.44 kN to 7.86 kN, corresponding to approximately 31 %, whereas the mean shear peak load decreased from 19.26 kN to 13.73 kN, corresponding to approximately 29 %. The similar direction of the change under both loading modes suggests that the short-term outdoor exposure affected the load-transfer capacity of the PU–masonry joint rather than only one specific loading configuration. The exposure involved simultaneous temperature variation, precipitation, ambient moisture, and solar exposure. These actions can potentially affect the polymer adhesive itself, the adhesive–masonry interface, or both. Moisture may influence the polymer network and interfacial adhesion, while temperature fluctuations may modify adhesive stiffness and stress transfer at the interface. Previous studies have reported changes in the mechanical properties of structural polyurethane adhesives following hygrothermal and outdoor ageing [11], while temperature-dependent changes in the adhesion of PU foam to masonry products have also been observed [12]. However, the present exposure was not designed to isolate individual environmental actions. Solar irradiance and moisture content of the masonry or adhesive were not measured directly, and only three specimens were tested per series. Therefore, the observed reductions cannot be attributed to a specific degradation mechanism. The results should instead be interpreted as preliminary evidence that the investigated PU-bonded masonry system is sensitive to combined short-term natural environmental exposure. Longer-term exposure, controlled hygrothermal conditioning, and larger specimen series are required to distinguish the contribution of individual environmental actions.

4. CONCLUSIONS

This study experimentally investigated the tensile and shear behaviour of polyurethane (PU) foam joints in masonry, with particular emphasis on the influence of short-term natural environmental exposure on their mechanical performance. The experimental programme included specimens maintained under controlled laboratory conditions and specimens exposed to unsheltered natural outdoor conditions for 33 days.

The obtained results demonstrated that PU foam joints exhibit a highly nonlinear mechanical response under both tensile and shear loading, characterised by an initial increase in load-bearing capacity followed by progressive softening after reaching the peak load. Based on the mean of the individual specimen peak loads, the exposed series exhibited a reduction of approximately 31 % in the tensile tests and 29 % in the shear tests compared with the corresponding reference series. These results indicate lower load-bearing capacity following the combined short-term outdoor exposure. Because only three specimens were tested per series, the observed differences are interpreted descriptively and should not be considered evidence of statistical significance.

Overall, the presented results contribute to a better understanding of the mechanical performance and short-term environmental sensitivity of polyurethane foam joints in masonry systems. Longer exposure periods, accelerated ageing procedures, and larger specimen series are required before conclusions can be drawn regarding long-term durability or the contribution of individual environmental actions.



(a) Reference series (b) Exposed series (c) Mean curves

Figure 12. Results of shear tests processed using DIC.

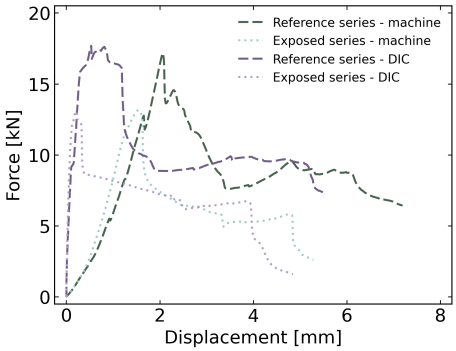


Figure 13. Comparison of the mean force–displacement curves obtained from the testing machine and DIC analysis for the reference and exposed series.

5. LIMITATIONS OF THE STUDY

The presented study has several limitations that should be clearly acknowledged. The experimental programme was limited to a single type of PU foam adhesive and one type of masonry unit. Therefore, the obtained conclusions cannot be generalised to all polyurethane-based masonry adhesives or all masonry systems without additional experimental verification. The number of specimens was limited to three per series; consequently, the comparison is primarily descriptive, and the observed variations in peak load values should be interpreted with caution. Furthermore, the shear tests were affected by local rotations and unavoidable eccentricities during loading, which could not be completely eliminated despite the applied restraints. These effects may have influenced the stress distribution within the adhesive layer and contributed to the irregularities observed in certain force–displacement responses, particularly in the post-peak phase. The effective bonded areas used for stress calculation were estimated from the observed adhesive footprint and the known perforated block geometry; individual bonded areas were not measured separately for every specimen, and some specimen-to-specimen variability is therefore expected.

Environmental exposure introduced an additional level of complexity to the mechanical behaviour of the investigated PU foam joints. However, it should be emphasised that the exposure period considered in this study was relatively short (33 days) and therefore primarily reflects short-term environmental effects. Consequently, further investigations involving longer exposure durations or accelerated ageing procedures are necessary in order to obtain a more comprehensive assessment of the long-term durability of PU foam adhesive joints.

Therefore, the presented results should be regarded as preliminary, since the experimental programme was limited in scope with respect to the number of specimens and duration of environmental exposure, while the testing procedures and experimental setup should be further improved and refined in future investigations. This will be addressed as part of the planned future research activities.

AUTHORS' CONTRIBUTION

Erik Kovaček: Investigation, Data curation, Formal analysis, Visualization, Writing – original draft.

Emina Hadžalić: Methodology, Investigation, Formal analysis, Validation, Writing – original draft, review and editing.

Nina Čeh: Conceptualization, Methodology, Supervision, Project administration, Funding acquisition, Writing – review and editing.

ACKNOWLEDGMENT

This work has been supported by the Croatian Science Foundation under project Resilient Engineering of Ductile Bonded Masonry: Understanding Dynamic Behavior and Seismic Response Across Scales (ResiBOND, HRZZ-UIP-2025-02-2749), Croatia.

REFERENCES

[1] A. N. Fried, J. J. Roberts, M. C. Limbachiya, A. Ahmed, Thin joint masonry in the UK, Masonry International, vol. 18, 2005, no. 2, pp. 85–87.

[2] N. Walliman, B. Baiche, R. Ogden, Thin-joint glued brickwork: Building in the British context, Construction and Building Materials, vol. 22, 2008, no. 6, pp. 1081–1092. DOI: 10.1016/j.conbuildmat.2007.03.008

[3] O. J. Kanyeto, A. Fried, Flexural behaviour of thin joint concrete blockwork: Experimental results, Construction and Building Materials, vol. 25, 2011, no. 8, pp. 3639–3647. DOI: 10.1016/j.conbuildmat.2011.03.059

[4] G. I. Grinfeld, A. S. Gorshkov, N. I. Vatin, Tests results strength and thermophysical properties of aerated concrete block wall samples with the use of polyurethane adhesive, Advanced Materials Research, vol. 941–944, 2014, pp. 786–799. DOI: 10.4028/www.scientific.net/AMR.941-944.786

[5] A. Jäger, E. Habian, M. Kasa, C. Kuhlemann, S. Lu, Verklebung von Planziegelmauerwerk mit Polyurethanklebern, Mauerwerk, vol. 15, 2011, no. 4, pp. 223–231. DOI: 10.1002/dama.201100504. [In German]

[6] M. Graubohm, W. Brameshuber, Investigations on the gluing of masonry units with polyurethane adhesive, Proceedings of the 8th International Masonry Conference, Dresden, Germany, 2010, pp. 287–295.

[7] D. Foti, M. Lerna, V. Vacca, Experimental characterization of traditional mortars and polyurethane foams in masonry wall, Advances in Materials Science and Engineering, vol. 2018, 2018, p. 8640351.
DOI: 10.1155/2018/8640351

[8] W. Brameshuber, M. Graubohm, Prefabricated masonry panel system with two-component polyurethane adhesive/Vorgefertigte Mauertafeln mit Zweikomponenten-Polyurethanklebstoff, Mauerwerk, vol. 19, 2015, no. 1, pp. 3–26.
DOI: 10.1002/dama.201500644

[9] E. Sudoł, E. Kozikowska, Mechanical properties of polyurethane adhesive bonds in a mineral wool-based external thermal insulation composite system for timber frame buildings, Materials, vol. 14, 2021, no. 10, p. 2527.
DOI: 10.3390/ma14102527

[10] S. P. Josyula, S. Diebels, Numerical investigation of fracture behaviour of polyurethane adhesives under the influence of moisture, Polymers, vol. 16, 2024, no. 18, p. 2676.
DOI: 10.3390/polym16182676

[11] J. M. Sousa, J. R. Correia, S. Cabral-Fonseca, Some permanent effects of hygrothermal and outdoor ageing on a structural polyurethane adhesive used in civil engineering applications, International Journal of Adhesion and Adhesives, vol. 84, 2018, pp. 406–419.
DOI: 10.1016/j.ijadhadh.2018.04.010

[12] V. Derkach, The influence of temperature impact on the strength of adhesion of polyurethane glue-foam with masonry products, E3S Web of Conferences, 2020, vol. 212, p. 02006.
DOI: 10.1051/e3sconf/202021202006

[13] J. A. Thamboo, M. Dhanasekar, Characterisation of thin layer polymer cement mortared concrete masonry bond, Construction and Building Materials, vol. 82, 2015, pp. 71–80.
DOI: 10.1016/j.conbuildmat.2014.12.098

[14] H. Schreier, J.-J. Orteu, M. A. Sutton, Image Correlation for Shape, Motion and Deformation Measurements: Basic Concepts, Theory and Applications, Springer, New York, 2009.
DOI: 10.1007/978-0-387-78747-3

[15] L. Collin, F. Gatuingt, C. Giry, F. Hild, Identification of non linear parameters from masonry triplet shear tests using digital image correlation, Materials and Structures, vol. 59, 2026, p. 193.
DOI: 10.1617/s11527-026-03052-1